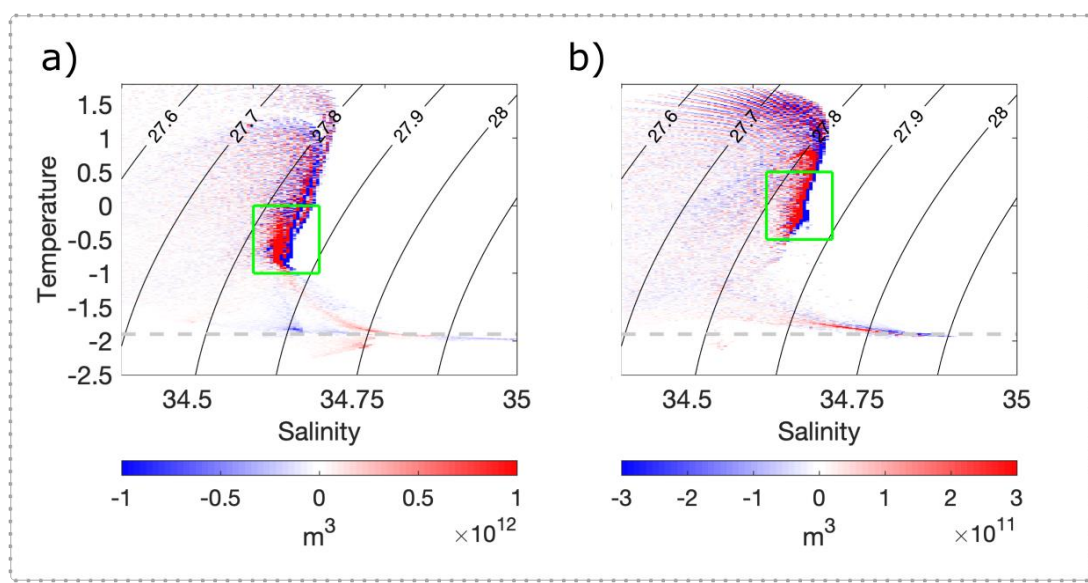


897

## Supplementary Figures

898



899

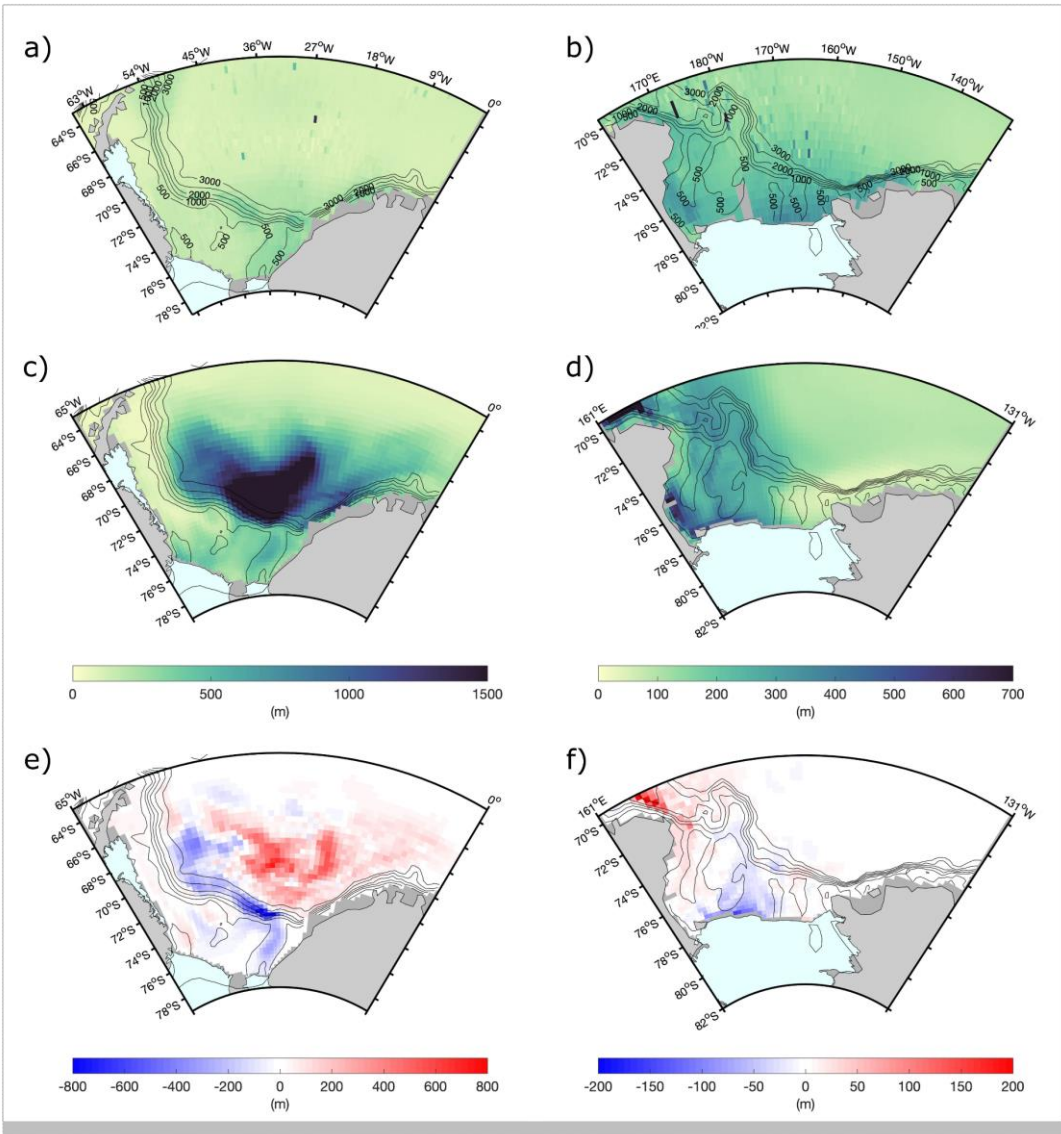
900

901

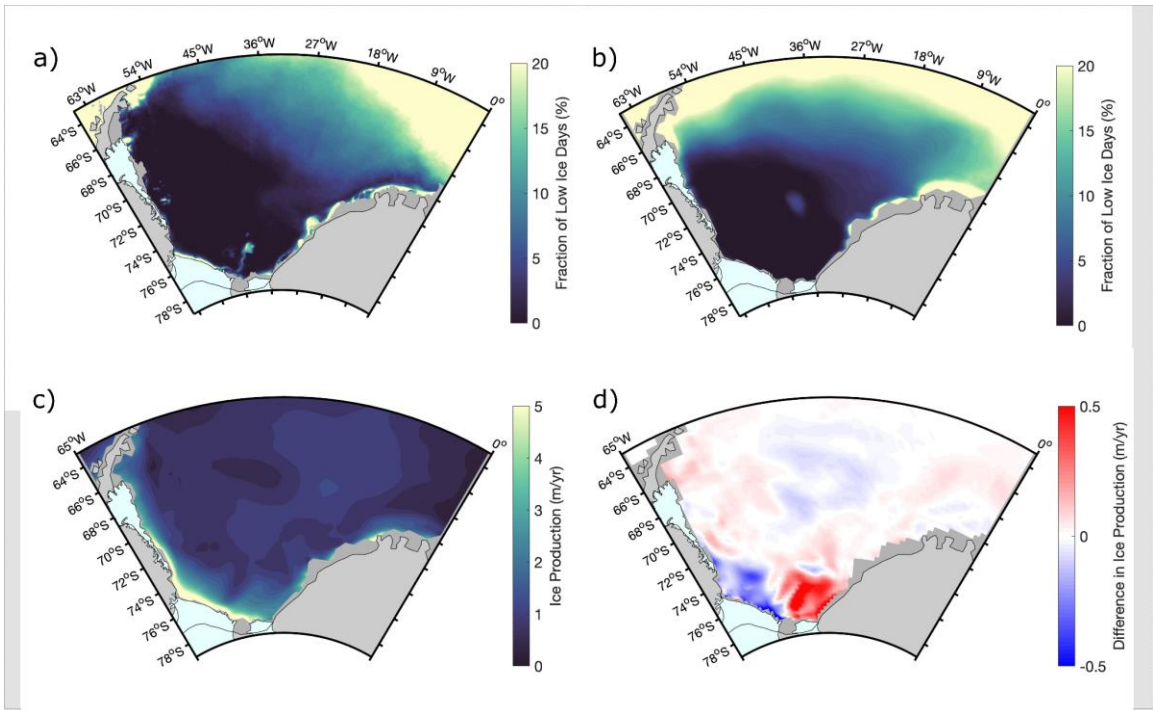
902

903

Supplementary figure 1: Difference (“Open” - “Closed”) in volumetric temperature versus salinity distributions for (a) the Weddell Sea ( $80^{\circ}\text{S}$ - $60^{\circ}\text{S}$  ;  $65^{\circ}\text{W}$ - $20^{\circ}\text{E}$ ) and (b) the Ross Sea ( $85^{\circ}\text{S}$ - $68^{\circ}\text{S}$ ;  $130^{\circ}\text{W}$ - $160^{\circ}\text{E}$ ) for model output excluding data underneath the ice shelves. The green boxes delimit the properties corresponding to AABW.

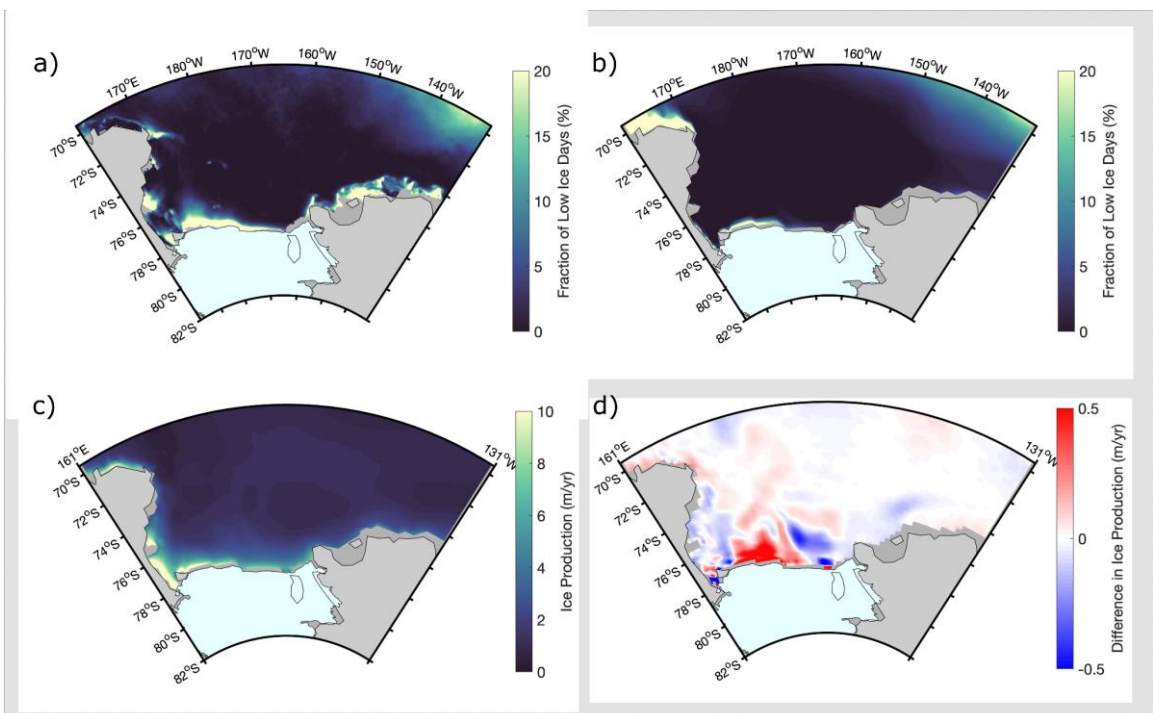


904  
905  
906 Supplementary Fig. 2: Winter mixed layer depths (MLD) from observational atlas of Sallee et al. (2021) shown in (a) and (b)  
907 for the Weddell and Ross Sea respectively, are compared with the winter mean from NEMO v4.2 eORCA1 forced model  
908 reference configuration equivalent years 1971-2009 in (c) and (d). The differences in MLDs between the “Open” cavity run  
909 and reference “Closed” run are shown in subplots (e) and (f).  
910



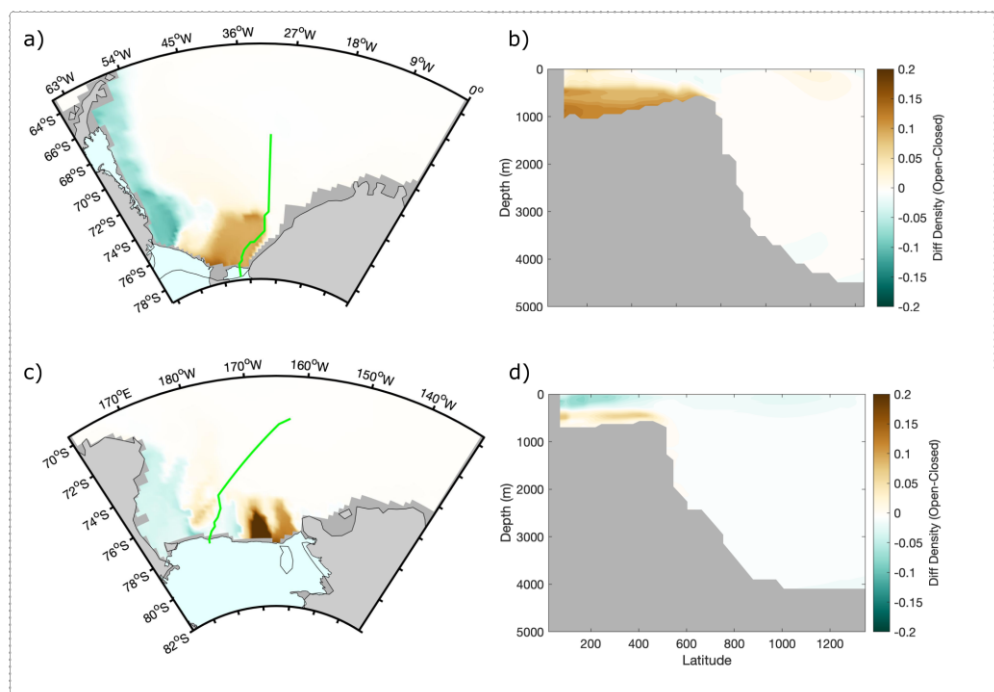
911  
912  
913  
914  
915  
916  
917

Supplementary Fig. 3: The fraction of low ice days for the period 2003-2009 for (a) satellite AMSR observations (Melsheimer et al., 2020) and (b) the NEMO "Closed" cavity reference configuration. Plot (c) shows the annual mean ice production in NEMO "Closed" configuration and (d) shows the difference in ice production between the "Open" and "Closed" cavity run (Open-Closed).



918  
919  
920  
921

Supplementary Fig. 4: Same as S3 but for the Ross Sea



922  
923

924 Supplementary Fig. 5: Density (kg/m<sup>3</sup>) plots for the Weddell (a-b) and Ross (c-d) Seas with bottom density in subplots (a)  
925 and (c) and the cross sections of the Filchner and Challenger troughs illustrated by green lines shown in subplots (b) and (d).

## 927 Supplementary Material

### 929 S1 An evaluation of ice production and polynya activity in the NEMO simulations

#### 931 S1.1 Scope

933 Sea ice growth, melt and drift exert an influence on water mass properties, according to many observational and model  
934 studies. In particular, near the Ronne and Ross ice shelf margins of interest for this study, during the cold season, large  
935 polynyas source dense saline waters to the surface ocean. In this Supplementary Material, we provide an evaluation of  
936 polynya activity in these two locations from our simulations and address: (i) how realistic polynya activity is; (ii) how  
937 polynya activity changes in response to the opening of cavities; and (iii) how associated changes in polynya activity affect  
938 biases in simulated water mass properties.

#### 940 S1.2 Methods

942 As an observational basis, we use the daily ice concentration 6.25 km resolution AMSR-E ASI product (Melsheimer and  
943 Spreen, 2020), best suited to the study of polynyas with its high resolution and daily coverage. From this, following Massom  
944 et al (1998), we diagnose annual polynya activity from the *fraction of low-ice days*, namely the fraction of days with ice  
945 concentration < 75 % over a 180-day period (days 91-270, i.e. April-September). From annual values, we compute the 2003-  
946 2009 mean, mapped in Figs. S3a and S4a for Weddell and Ross Sea regions, respectively.

947 We compute a comparable diagnostic from model daily ice concentration outputs, whose 2003-2009 average in the “Closed”  
948 simulation is mapped in Figs. S3b and S4b.

949 We supplement these diagnostics with simulated annual ice production, computed as the total volume of ice produced per  
950 unit area each year. Figs. S3c and S4c map 2003-2009 averages for the “Closed” simulation and Figs. S3d and S4d show the  
951 “Open”-“Closed” difference.

952 We also calculate yearly ice production summed over each polynya region and compare the results with observational  
953 counterparts in the Supplementary Table below.

Ice production (10 <sup>9</sup> m <sup>3</sup> )	Nakata et al. (2021)	Closed	Open
Ronne Polynya	58 ± 21	24	29
Ross + Terra Nova Bay Polynya	387 ± 41	368	357

959 Supplementary table 1: Comparison between observational estimates and the NEMO eORCA1 configuration “Closed” and  
960 “Open” cavity runs for net ice production in Ronne Polynya of the Weddell Sea and the sum of Ross and Terra Nova Bay  
961 polynyas of the Ross Sea.

962

### 963 S1.4 Evaluating polynya activity

964

965 The observed fraction of low ice days indicates polynya activity at the expected locations (see, e.g., Nakata et al, 2021). In  
966 the Weddell Sea, this includes the Ronne Polynya off Ronne Ice Shelf (Fig. S3a); in the Ross Sea, this includes the Ross and  
967 Terra Nova Bay polynyas (Fig. S4a) and smaller polynyas further north. This corresponds to where we observe hyper-saline  
968 bottom waters (Figs. 2f and 3f).

970 Unlike observations, the simulated fraction of low ice days shows no apparent polynya activity along the ice-shelf fronts  
971 (Figs. S3b and S4b). We argue that this discrepancy is due to inconsistencies between the way the model and observations  
972 define ice concentration. Indeed, in the model, sea ice drift (aka *dynamics*), then growth and melt (aka *thermodynamics*) are  
973 calculated sequentially, at each time step. In this context, any dynamically-driven opening in the ice is, under the action of  
974 sufficiently cold air, instantaneously frozen by model thermodynamics, with thin ice. Such thin ice contributes to ice  
975 concentration as ice of any thickness, explaining why simulated concentration can be nearly 100 % in polynya regions.  
976 Satellite retrievals of ice concentration possess inherent differences with model estimates. First they have much higher  
977 resolution. Second, they contrast thick ice and open water fairly well and do not suffer from the closing effect described  
978 above. All this contributes to lower ice concentration in polynya regions in satellite products as compared with NEMO  
979 output. An additional contributing factor might be that thin ice and open water are hard to distinguish, such that some thin  
980 ice might be counted as open water in satellite products, as has been shown to occur for at least some sea ice passive  
981 microwave (PMW) algorithms (Kern et al., 2022).

982

983 From simulated ice production, Ronne (Fig. S3c), Ross and Terra Nova Bay (Fig. S4c) polynyas have a clear signature in the  
984 model, at the approximate locations inferred from the observed low-ice-day fraction. Fairly similar patterns are seen in  
985 simulated ice thickness fields (not shown), with very thin (<25 cm) ice found where polynas are deemed active. For these  
986 reasons, we surmise that there are active polynyas in our simulations, but that the fraction of low-ice days is a poor  
987 diagnostic for their identification. Instead, ice production captures the polynya activity and most importantly reflects their  
988 impact on water-mass transformation.

989

990 Annual ice production maps also indicate possible errors in the distribution of simulated polynya activity. In particular, the  
991 Ross Sea Polynya seems too narrow, whereas the Terra Nova Bay polynya seems too wide, especially north of McMurdo  
992 Sound, possibly due to the lack of landfast ice in the simulations north of McMurdo Sound (Fraser et al., 2021).

993

994 Annually-integrated ice production in the Ronne Polynya under-estimates observations. By contrast, ice production in the  
995 Ross and Terra Nova Bay polynyas is consistent with the observational estimate, though the simulated production rate is  
996 based on too large an area.

997

### 998 S1.5 Effect of opening cavities on polynya activity

999

1000 Opening cavities is associated with changes in ice production close to the polynya regions. Overall, the annually integrated  
1001 ice production (Supplementary Table 1) only slightly changes because the net effect is a residual between roughly equal

1002 areas of ice production decrease (to the west of the ice shelves) and increase (to the east of the ice shelves). It is hard to  
1003 conclude on more or less realistic polynya activity in the “Open” simulation.

1004  
1005 Changes in ice production due to opening cavities are largely consistent with patterns of temperature and salinity  
1006 adjustments. Ice production is lower where temperature is higher and salinity is lower. This is consistent with circulation-  
1007 induced ocean temperature changes forcing an alteration in ice production, with possible feedback on salinity. In the  
1008 Weddell Sea, a re-organisation of the shelf circulation to subduct HSSW under the ice shelf reduces the ice production in the  
1009 Ronne Depression and increases it to the east over the Filchner Trough. The pattern of sea ice change in the Ross Sea is less  
1010 homogeneous east-west, with a reduction in Terra Nova Bay and in front of Roosevelt Island and an increase in sea ice over  
1011 the Challenger Trough which is where ice shelf water (ISW) is exported.

1012  
1013 **S1.6 Summary**

1014  
1015 In summary, ice production in polynya regions decreases west of the ice shelves and mostly increases east of them when  
1016 opening cavities. The decrease to the west may contribute to a reduction of the high salinity bias there. On the eastern side,  
1017 increased ice production and brine rejection combines with northward export of cold ISW from the under-ice cavities. The  
1018 resultant effect in the Weddell Sea is a strong east-west temperature and salinity difference (Fig. 2i). In the Ross Sea, on the  
1019 other hand, increased brine rejection seems compensated by anomalous export of relatively fresh water from under the ice  
1020 shelf (Fig. 3i).

1021  
1022 **Data**

1023  
1024 The AMSR-E ASI sea ice concentration data used can be found at: <https://doi.pangaea.de/10.1594/PANGAEA.919778>

1025  
1026 **Bibliography**

1027  
1028 Nakata, K., Ohshima, K. I. and Nihashi, S.: Mapping of active frazil for Antarctic coastal polynyas, with an estimation of  
1029 sea-ice production, Wiley Online Library, 2021.

1030  
1031 Melsheimer, C. and Spreen, G.: AMSR-E ASI sea ice concentration data, Antarctic, version 5.4 (NetCDF) (June 2002 -  
1032 September 2011), <https://doi.pangaea.de/10.1594/PANGAEA.919778>, 2020.

1033  
1034 Massom, R. A., Harris, P. T., Michael, K. J. and Potter, M. J.: The distribution and formative processes of latent-heat  
1035 polynyas in East Antarctica, Cambridge University Press, 1998.

1036  
1037 Fraser, A. D., Massom, R. A., Handcock, M. S., Reid, P., Ohshima, K. I., Raphael, M. N., Cartwright, J., Klekociuk, A. R.,  
1038 Wang, Z. and Porter-Smith, R.: Eighteen-year record of circum-Antarctic landfast-sea-ice distribution allows detailed  
1039 baseline characterisation and reveals trends and variability, Copernicus GmbH, 2021.

1040  
1041 Kern, S., Lavergne, T., Pedersen, L. T., Tonboe, R. T., Bell, L., Meyer, M. and Zeigermann, L.: Satellite passive microwave  
1042 sea-ice concentration data set intercomparison using Landsat data, Copernicus GmbH, 2022.